

Auophilic Interactions Studied by Quantum Crystallography

Sylwia Pawłędzio, Maura Malinska, Florian Kleemiss, Simon Grabowsky, and Krzysztof Woźniak*

Cite This: <https://doi.org/10.1021/acs.inorgchem.1c03333>

Read Online

ACCESS |



Metrics & More



Article Recommendations



Supporting Information

ABSTRACT: This is the first use of a wave-function-based crystallographic method to characterize auophilic interactions from X-ray diffraction data. Theoretical calculations previously suggested the importance of electron correlation and dispersion forces, but no influence of relativistic corrections to the Au...Au interaction energy was found. In this study, we confirm the importance of relativistic corrections in the characterization of auophilic interactions in addition to electron correlation and dispersion.

Auophilic interactions^{1–3} refer to weak metallophilic contacts^{4–7} formed between gold atoms with 5d¹⁰ closed-shell valence electron configuration. They occur as *intra-* or *intermolecular* noncovalent interactions (NCIs) and significantly influence the molecular and crystal structures. They are responsible for unusual aggregations of molecules,⁸ such as, e.g., dimers, trimers, chains, or layers, with short Au...Au distances.⁹ The presence of auophilic interactions results in the appearance of specific materials properties, including catalytic properties,¹⁰ electric conductivity,¹¹ or luminescence.^{12–14}

In all types of metallophilic interactions, the metal–metal distance is shorter than the sum of the van der Waals radii, which is associated with a decrease in the bond energy,^{15,16} comparable to hydrogen or halogen bonds, π – π stacking, and other weak interactions. Generally, metallophilic interactions are formed between metals with low coordination numbers,¹⁷ typically heavy elements. Therefore, these types of interactions are not only dominated by orbital,^{11,18} electrostatic,^{11,18} and dispersion forces¹⁷ but also benefit from relativistic effects.^{19,20} At the bottom of the periodic table, relativistic effects are maximal for gold,²¹ and thus the strongest metallophilic interactions are observed for Au...Au contacts.^{22–24}

Noncovalent forces play a crucial role in determining both the shape of the molecular structure and the supramolecular architecture of crystals.²⁵ A key application of quantum crystallography^{26,27} is to understand the nature of intermolecular NCIs in crystals, going beyond the analysis of geometrical parameters. In that sense, an essential source of information is the electron density, which can be obtained from X-ray diffraction (XRD) experiments and described using quantum mechanical principles and concepts. The quantum crystallographic method utilized here is Hirshfeld atom refinement (HAR; Table 1).^{28,29} HAR is a wave-function-based procedure for modeling diffraction data. Structural parameters, namely atomic positions and their anisotropic displacement parameters (ADPs), are obtained from XRD experiments in an iterative procedure, where cycles of either Hartree–Fock (HF) or density functional theory (DFT) calculations of molecular electron density partitioned into aspherical atoms and least-squares refinement are repeated

Table 1. Structure Refinement Details^a

	IAM	HAR
data/restraints/param	2042/0/48	2042/0/95
GOF on F ²	1.198	0.924
final R indices (all data)	R ₁ = 2.52%, wR ₂ = 6.93%	R ₁ = 2.18%, wR ₂ = 6.08%
largest diff peak/hole (e/Å ³)	2.54/−4.17	1.91/−1.65

^aFinal R indices are provided for the IAM and HAR (rks_anh_rel) models refined in SHEXL and NoSpherA2, respectively.

until convergence. Since the electron density is not refined in HAR but calculated at a high level of theory, the experimentally obtained atomic positions and ADPs from HAR refinement are more accurate and precise than any others.^{29,30} Quantum Crystallography has already been successfully applied to structures containing heavy metals, where the influence of the relativistic effects, electron correlation, and anharmonicity on the electron density distribution in crystals has been confirmed and characterized in detail.^{31–34}

In practice, theoretical characterization of metallophilic interactions is very difficult because of the complex chemistry of heavy atoms and the lack of accurate experimental references.^{35–37} Thus, the binding energies of auophilic interactions have been the subject of many theoretical studies at several levels of theory, including DFT, second-order Møller–Plesset (MP2), and coupled cluster singles doubles (triples) [CCSD(T)] methods.^{36,38} It was found that MP2 tends to overestimate the interaction energies with respect to the CCSD(T) reference method.³⁶ On the other hand, DFT can only give reasonable dimer energies when a dispersion correction is applied.^{35,39,40}

Received: October 25, 2021

The aim of the present study is to accurately characterize aurophilic interactions present in a crystal structure of chloro(dimethyl sulfide)gold (Figure 1a) by using the HAR

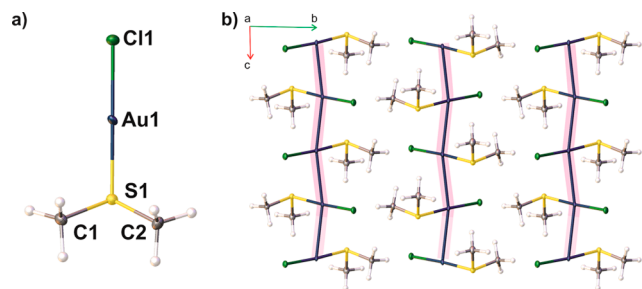


Figure 1. (a) Molecular structure of Cl–Au–S(CH₃)₂ after HAR with the labeling scheme. Ellipsoids are drawn with 50% probability. (b) Crystal packing along the [100] crystallographic direction showing aurophilic interactions (highlighted in pink).

method, as implemented in *NoSpherA2*.⁴¹ The effects of relativity (REL) and electron correlation (ECORR) on the electron density distribution along the Au...Au contact are the main focus of this work. We looked in-depth into the interaction energies, the Quantum Theory of Atoms in Molecules (QTAIM)⁴² parameters at bond critical points (BCPs), and the negative Laplacian profiles of the Cl–Au–S(CH₃)₂ dimer (Figure 2) for the theoretical electron densities

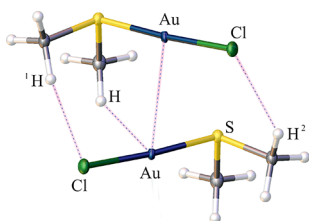


Figure 2. Molecular structure of the investigated Cl–Au–S(CH₃)₂ dimer with intermolecular contacts detected within QTAIM analysis. Symmetry codes: 1, *x*, *y*, *z*; 2, *x*, 1.5 – *y*, 0.5 + *z*.

at the HAR geometries calculated at different levels of theory. The present work is a first attempt at using the wave-function-based method HAR for a description of aurophilic interactions—using its experimental geometry as well as analyzing the wave function used in the refinement.

The structure of chloro(dimethyl sulfide)gold⁴³ was reinvestigated by collecting the XRD data at the SPring-8 synchrotron station in Japan (beamline BL02B1). The investigated compound crystallized in the monoclinic *P*2₁/*c* space group with one molecule in the asymmetric unit. All further information about the compound can be found in the Supporting Information (SI). HARs were performed at HF-DKH2/*x*2c-TZVPPall (rhf_anh_rel, Table 1), B3LYP-DKH2/*x*2c-TZVPPall (rks_anh_rel, Table 1), and B3LYP/*x*2c-TZVPPall (rks_anh_nrel). The abbreviation anh refers to the inclusion of anharmonic motion refinement. Empirical dispersion corrections are irrelevant to the electron density underlying HAR; they are only important for calculation of the energies.⁴⁴

The Cl–Au–S atoms are in an exceptional linear geometry, 176.63(2)°, which leaves the coordination sphere of the gold atom open. Molecules form an infinite Au...Au...Au chain in the crystal lattice, along the *c* crystallographic axis (Figure 1b)

with a Au...Au...Au valence angle of 167.24(1)°. Adjacent molecules in each Au...Au...Au chain, highlighted in pink (Figure 1), are trans-arranged to each other, with the Cl–Au–S line almost perpendicular to the chain. The Au...Au distance has a typical value of 3.15983(6) Å. The aurophilic interaction energy computed at the B3LYP/*x*2c-TZVPPall level with empirical dispersion and basis set superposition error corrections at the fixed molecular geometry obtained in HAR (Figure 2) was predicted to be attractive by 67.74 kJ/mol (Table 2).

Table 2. Interaction Energies (kJ/mol) for the Cl–Au–S(CH₃)₂ Dimer Using the *x*2c-TZVPPall Basis Set with Counterpoise Correction at Different Levels of Theory

HF-DKH2	2.93
B3LYP-GD3BJ	–67.36
B3LYP-GD3BJ-DKH2	–67.74
B3LYP-DKH2	–12.09

This value seems to be independent of relativistic corrections (B3LYP-GD3BJ-DKH2 vs B3LYP-GD3BJ) but strongly changed when dispersion (B3LYP-DKH2) or electron correlations (HF-DKH2) were neglected. The former reduces the attractive character of the interaction energy, while the latter even makes it repulsive. The studied structure also forms other noncovalent contacts.⁴⁵ More details are given in the SI.

QTAIM was applied to analyze the quantum-mechanical electron density available after HAR. The BCPs and bond paths (Tables S10–S12 and Figure S7) confirm the existence of all covalent bonds as well as C–H...Cl, C–H...Au, and Au...Au intermolecular contacts (Figure 2). Tables 3 and S9 present the QTAIM parameters characterizing the BCPs obtained for the above-mentioned intermolecular contacts at different levels of theory.

For all contacts present in Tables 3 and S9, the small values of the electron densities, together with the small and positive values of the corresponding Laplacian, indicate closed-shell interactions. However, the negative sign of the potential energy densities V_r denotes a stabilizing character of the investigated contacts upon electron sharing. This is confirmed by the delocalization index (DI), which is the average number of electron pairs shared between two atomic basins (Tables 3 and S9). The largest values of the DI among all intermolecular contacts present in the Cl–Au–S(CH₃)₂ dimer are found for the aurophilic interactions, indicating their stabilizing character. Stabilization of the Au...Au contact increases when relativistic effects and electron correlation are included (Table 3, model rks_anh_rel), while for Au...H and Cl...H interactions, the influence of these corrections is marginal (Table S9). Within the rks_anh_rel model, a decrease of the total energy density [$H_r/\rho(r)$] to a negative value is observed, and, consequently, some covalent character of the Au...Au contact is detected. Hence, the relativistic effects are a key factor influencing the character of the aurophilic interactions shown in both the DI and $H_r/\rho(r)$ parameters. The same trend is observed with regard to the $|V_r|/G_r$ ratio, which is more sensitive to relativistic effects than the electron correlation correction.⁴⁶ A value > 1 indicates an intermediate strength for an Au...Au interaction.

Electron-density analysis also sheds light on the Au...Au interaction in a more global way. This is shown in Figures 3 and S8 where the distribution of the electron density and its

Table 3. QTAIM Parameters at BCPs for Contacts Present in the Cl–Au–S(CH₃)₂ Dimer and DI Computed between Two Atomic Basins

contact	method	$\rho(r)$ (e/Å ³)	$\nabla^2\rho(r)$ (e/Å ⁵)	V_r (hartree)	$H_r/\rho(r)$ (hartree/e)	$ V_r /G_r$	DI
Au...Au	rks_anh_rel	0.160	1.398	−0.016	−0.029	1.046	0.25
	rks_anh_nrel	0.125	1.133	−0.011	0.015	0.975	0.16
	rhf_anh_rel	0.140	1.502	−0.015	0.010	0.986	0.18

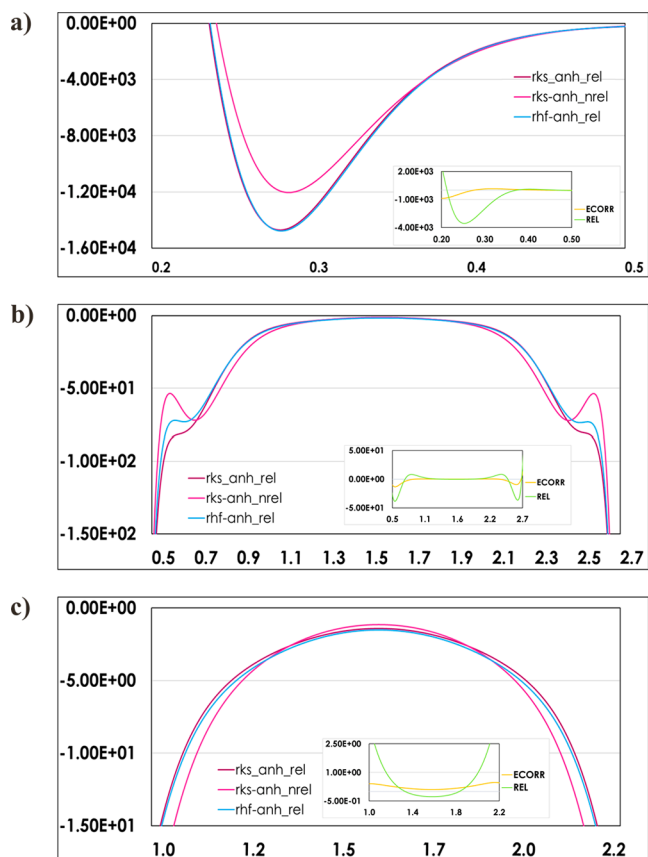


Figure 3. 1D plots of negative Laplacian (y axis, in e/Å⁵) as a function of the Au...Au contact distance (x axis, in Å) for theoretical electron densities used in the HAR models, showing the most interesting changes in their courses in terms of magnifications of different bonding ranges. The subplots show differences of the negative Laplacian resulting from the relativistic (REL) and electron correlation (ECORR) effects obtained as a result of subtraction of the rel_anh_rel–rks_anh_nrel and rks_anh_rel–rhf_anh_rel models, respectively.

negative Laplacian along the Au...Au contact at different levels of theory are presented. The impact of ECORR and REL is shown in the subplots as subtraction of the rks_anh_rel–rhf_anh_rel and rel_anh_rel–rks_anh_nrel models. Similar to the covalent bonds,^{32,34} the differences between the models are visible. However, the dominant role of ECORR over REL, with regard to the electron density, is only detected in the region of 0.3–0.6 Å (Figure S8).

The ECORR and REL corrections also influence the shapes of the negative Laplacian profiles. The first difference is visible in the region of local charge depletion (the 0.25–0.35 Å range). Compared to the covalent bonds,³⁴ the magnitudes of these minima deviate by ca. 300 and 250 e/Å⁵ for REL and ECORR, respectively, with a shift of the charge depletion minimum due to a relativistic contraction of 0.01 Å. Furthermore, the local charge concentration in the region of

0.5–0.7 Å is the highest for the rks_anh_nrel model (Figure 3). This means that the reduction of the electron density concentration in this region is mainly caused by relativistic effects (similar to the previously reported study for covalent bonds –subplots in Figure 3a): the magnitudes of the local maxima for the Au...Au interaction in this region are half the amounts previously reported for the covalent Au–P and Au–C bonds.³⁴ On the other hand, contrary to the covalent bonds, the dependence of the curve of the negative Laplacian on the distance in the bonding region for the Au...Au interaction (1.2–2.0 Å) is even more affected by REL (subplots in Figure 3b) than by ECORR.

We have shown that the energy of the dimer is mostly dominated by weak dispersion forces, which are mainly associated with the existence of C–H...Cl, C–H...Au, and C–S...Au contacts and partly enhanced by attractive forces of the Au...Au interaction. Through counterpoise calculations, we have also shown the importance of electron correlation effects on the resulting dimer energy value, which seemed to be independent of the relativistic correction. However, within QTAIM analysis, performed at different levels of theory, we have stressed the importance of both electron correlation and relativistic corrections in the characterization of aurophilic interactions. Within a QTAIM analysis, we have identified an intermediate closed-shell type of aurophilic interaction with some features of covalency but only when REL and ECORR corrections were applied together. Importantly, REL changes the electron density distribution more than ECORR correction. It enhances the stabilization of the Au...Au interactions and their covalent character. The above-mentioned observations correspond well with previously reported studies.^{22,33} Here, we were able to distinguish the significance of dispersion forces and relativistic corrections in terms of dimer energy and electron density properties, respectively.

Dispersion is very important for accurate dimer energy estimation. However, the dimer energy results from all interactions and close contacts present in the dimer, for which other weak contacts such as C–H...Cl, C–H...Au, and C–S...Au prevail over aurophilic interactions. On the other hand, the relativistic correction enhances the covalent character of the Au...Au interaction, which is reflected in the electron density properties.

Relativistic effects strongly dominate the metal core region also in the direction of the NCIs and all of the valence and bonding regions with regard to the metal...metal interaction. Our findings emphasize the computational challenge in the characterization of metal...metal NCIs, in understanding aurophilic and other secondary interactions, and how quantum crystallography can be a very useful tool for deriving reliable bond characterizations for metallophilic interactions.

A geometry optimization for polymeric structures with heavy elements in periodic conditions, with an all-electron basis set, is still a challenge for theoretical chemistry, and thus the geometry obtained by an XRD experiment is very important.

This seems to be a great solution in this case because we are able to combine both experimental data (which characterized the geometry in periodic conditions) and theoretical calculations to investigate such difficult crystal structures.

■ ASSOCIATED CONTENT

SI Supporting Information

The Supporting Information is available free of charge at <https://pubs.acs.org/doi/10.1021/acs.inorgchem.1c03333>.

X-ray data collection details, histogram and frequency table for Au...Au interactions, ADPs, bond lengths and valence angles, Hirshfeld surface and NCI analysis, relative contributions of different intermolecular contacts to the Hirshfeld surface, 2D fingerprint plots for the Hirshfeld surface, NCI isosurfaces ($s = 0.3$ au) for the investigated dimer, HAR refinement details, effects of a different basis set used in HAR, QTAIM parameters at the BCPs at different levels of theory, labeling scheme and molecular graphs for the investigated dimer, 1D plots of the electron density as a function of the length of the Au...Au contact, normal probability plots for tested models, anharmonic thermal motions analysis, and references (PDF)

Accession Codes

CCDC 2116322–2116325 contain the supplementary crystallographic data for this paper. These data can be obtained free of charge via www.ccdc.cam.ac.uk/data_request/cif, or by emailing data_request@ccdc.cam.ac.uk, or by contacting The Cambridge Crystallographic Data Centre, 12 Union Road, Cambridge CB2 1EZ, UK; fax: +44 1223 336033.

■ AUTHOR INFORMATION

Corresponding Author

Krzysztof Woźniak – Biological and Chemical Research Centre, Department of Chemistry, University of Warsaw, 02-089 Warszawa, Poland; orcid.org/0000-0002-0277-294X; Email: kwozniak@chem.uw.edu.pl

Authors

Sylvia Pawłędzio – Biological and Chemical Research Centre, Department of Chemistry, University of Warsaw, 02-089 Warszawa, Poland

Maura Malinska – Biological and Chemical Research Centre, Department of Chemistry, University of Warsaw, 02-089 Warszawa, Poland; orcid.org/0000-0002-7138-7041

Florian Kleemiss – Department of Chemistry, Biochemistry and Pharmaceutical Sciences, University of Bern, 3012 Bern, Switzerland; Faculty for Chemistry und Pharmacy, University of Regensburg, 93053 Regensburg, Germany

Simon Grabowsky – Department of Chemistry, Biochemistry and Pharmaceutical Sciences, University of Bern, 3012 Bern, Switzerland

Complete contact information is available at:

<https://pubs.acs.org/doi/10.1021/acs.inorgchem.1c03333>

Author Contributions

All authors have given approval to the final version of the manuscript

Funding

Support of this work by the National Science Centre, Poland, through PRELUDIUM Grant UMO-2018/31/N/ST4/02141 and the University's Integrated Development Programme

(ZIP), cofinanced by the European Social Fund within the framework of Operational Programme Knowledge Education Development 2016–2020, action 3.5, is gratefully acknowledged.

Notes

The authors declare no competing financial interest.

■ ACKNOWLEDGMENTS

The synchrotron radiation experiments were performed at BL02B1 of SPring-8 with the approval of the Japan Synchrotron Radiation Research Institute (Proposal 2019A1069). This research was supported, in part, by PL-Grid Infrastructure (Grant plgrozpoznanie 5). This work was partly carried out at the Biological and Chemical Research Centre, University of Warsaw, established within the project cofinanced by the European Union from the European Regional Development Fund under the Operational Programme Innovative Economy, 2007–2013. The work was accomplished at the TEAM TECH Core Facility for crystallographic and biophysical research to support the development of medicinal products sponsored by the Foundation for Polish Science (Grant 115). S.P. thanks Dr. hab. Anna Makal, Dr. Marcin Stachowicz, Dr. Kunihisa Sugimoto, and Daniel Tchoń for their assistance and support at the SPring-8 synchrotron station.

■ REFERENCES

- (1) Schmidbaur, H. Is Gold Chemistry a Topical Field of Study? *Angew. Chem. Int. Ed. Engl.* **1976**, *15* (12), 728–740.
- (2) Schmidbaur, H.; Graf, W.; Müller, G. Weak Intramolecular Bonding Relationships: The Conformation-Determining Attractive Interaction between Gold(I) Centers. *Angew. Chem. Int. Ed. Engl.* **1988**, *27* (3), 417–419.
- (3) Schmidbaur, H. The Auophilicity Phenomenon: A Decade of Experimental Findings, Theoretical Concepts and Emerging Applications. *Gold Bull.* **2000**, *33* (1), 3–10.
- (4) Pykkö, P.; Li, J.; Runeberg, N. Predicted Ligand Dependence of the Au(I)...Au(I) Attraction in (XAuPH₃)₂. *Chem. Phys. Lett.* **1994**, *218* (1), 133–138.
- (5) Schmidbaur, H.; Schier, A. Argentophilic Interactions. *Angew. Chem., Int. Ed.* **2015**, *54* (3), 746–784.
- (6) Schmidbaur, H.; Schier, A. Mercurophilic Interactions. *Organometallics* **2015**, *34* (11), 2048–2066.
- (7) Harisomayajula, N. V. S.; Makovetskyi, S.; Tsai, Y.-C. Cuprophilic Interactions in and between Molecular Entities. *Chem. Eur. J.* **2019**, *25* (38), 8936–8954.
- (8) Katz, M. J.; Sakai, K.; Leznoff, D. B. The Use of Auophilic and Other Metal–Metal Interactions as Crystal Engineering Design Elements to Increase Structural Dimensionality. *Chem. Soc. Rev.* **2008**, *37* (9), 1884–1895.
- (9) Jones, P. G. X-Ray Structural Investigations of Gold Compounds. *Gold Bull.* **1986**, *19* (2), 46–57.
- (10) Tkatchouk, E.; Mankad, N. P.; Benitez, D.; Goddard, W. A.; Toste, F. D. Two Metals Are Better Than One in the Gold Catalyzed Oxidative Heteroarylation of Alkenes. *J. Am. Chem. Soc.* **2011**, *133* (36), 14293–14300.
- (11) Zheng, Q.; Borsley, S.; Nichol, G. S.; Duarte, F.; Cockroft, S. L. The Energetic Significance of Metallophilic Interactions. *Angew. Chem., Int. Ed. Engl.* **2019**, *58* (36), 12617–12623.
- (12) Vickery, J. C.; Olmstead, M. M.; Fung, E. Y.; Balch, A. L. Solvent-Stimulated Luminescence from the Supramolecular Aggregation of a Trinuclear Gold(I) Complex That Displays Extensive Intermolecular Au...Au Interactions. *Angew. Chem. Int. Edit. Engl.* **1997**, *36* (11), 1179–1181.
- (13) Han, S.; Yoon, Y. Y.; Jung, O.-S.; Lee, Y.-A. Luminescence on–off Switching via Reversible Interconversion between Inter-

- Intramolecular Auophilic Interactions. *Chem. Commun.* **2011**, 47 (38), 10689–10691.
- (14) Glodek, M.; Pawłędzio, S.; Makal, A.; Plažuk, D. The Impact of Crystal Packing and Auophilic Interactions on the Luminescence Properties in Polymorphs and Solvate of Aroylacetylde–Gold(I) Complexes. *Chem. Eur. J.* **2019**, 25 (57), 13131–13145.
- (15) Pyykkö, P. Strong Closed-Shell Interactions in Inorganic Chemistry. *Chem. Rev.* **1997**, 97 (3), 597–636.
- (16) Bardaji, M.; Laguna, A. Gold Chemistry: The Auophilic Attraction. *J. Chem. Educ.* **1999**, 76 (2), 201.
- (17) Oлару, M.; Kögel, J. F.; Aoki, R.; Sakamoto, R.; Nishihara, H.; Lork, E.; Mebs, S.; Vogt, M.; Beckmann, J. Tri- and Tetranuclear Metal-String Complexes with Metallophilic d^{10} – d^{10} Interactions. *Chem. Eur. J.* **2020**, 26 (1), 275–284.
- (18) Oeschger, R. J.; Chen, P. A Heterobimetallic Pd–Zn Complex: Study of a d^8 – d^{10} Bond in Solid State, in Solution, and in Silico. *Organometallics* **2017**, 36 (8), 1465–1468.
- (19) Pyykkö, P. Relativistic Effects in Structural Chemistry. *Chem. Rev.* **1988**, 88 (3), 563–594.
- (20) Scherbaum, F.; Grohmann, A.; Huber, B.; Krüger, C.; Schmidbaur, H. Auophilicity as a Consequence of Relativistic Effects: The Hexakis(Triphenylphosphaneaurio)Methane Dication $[(Ph_3PAu)_6C]^{2+}$. *Angew. Chem. Int. Ed. Engl.* **1988**, 27 (11), 1544–1546.
- (21) Pyykkö, P.; Desclaux, J. P. Relativity and the Periodic System of Elements. *Acc. Chem. Res.* **1979**, 12 (8), 276–281.
- (22) Magnko, L.; Schweizer, M.; Rauhut, G.; Schütz, M.; Stoll, H.; Werner, H.-J. A Comparison of Metallophilic Attraction in $(X-M-PH_3)_2$ ($M = Cu, Ag, Au$; $X = H, Cl$). *Phys. Chem. Chem. Phys.* **2002**, 4 (6), 1006–1013.
- (23) Schmidbaur, H.; Schier, A. A Briefing on Auophilicity. *Chem. Soc. Rev.* **2008**, 37 (9), 1931–1951.
- (24) Schmidbaur, H.; Schier, A. Auophilic Interactions as a Subject of Current Research: An Up-Date. *Chem. Soc. Rev.* **2012**, 41 (1), 370–412.
- (25) Müller-Dethlefs, K.; Hobza, P. Noncovalent Interactions: A Challenge for Experiment and Theory. *Chem. Rev.* **2000**, 100 (1), 143–168.
- (26) Grabowsky, S.; Genoni, A.; Bürgi, H.-B. Quantum Crystallography. *Chem. Sci.* **2017**, 8 (6), 4159–4176.
- (27) Genoni, A.; Bučinský, L.; Claiser, N.; Contreras-García, J.; Dittrich, B.; Dominiak, P. M.; Espinosa, E.; Gatti, C.; Giannozzi, P.; Gillet, J.-M.; Jayatilaka, D.; Macchi, P.; Madsen, A. Ø.; Massa, L.; Matta, C. F.; Merz, K. M.; Nakashima, P. N. H.; Ott, H.; Ryde, U.; Schwarz, K.; Sierka, M.; Grabowsky, S. Quantum Crystallography: Current Developments and Future Perspectives. *Chem. Eur. J.* **2018**, 24 (43), 10881–10905.
- (28) Jayatilaka, D.; Dittrich, B. X-Ray Structure Refinement Using Aspherical Atomic Density Functions Obtained from Quantum-Mechanical Calculations. *Acta Crystallogr., Sect. A* **2008**, 64 (3), 383–393.
- (29) Capelli, S. C.; Bürgi, H.-B.; Dittrich, B.; Grabowsky, S.; Jayatilaka, D. Hirshfeld Atom Refinement. *IUCrJ.* **2014**, 1 (5), 361–379.
- (30) Sanjuan-Szklarz, W. F.; Wońska, M.; Domagała, S.; Dominiak, P. M.; Grabowsky, S.; Jayatilaka, D.; Gutmann, M.; Woźniak, K. On the Accuracy and Precision of X-Ray and Neutron Diffraction Results as a Function of Resolution and the Electron Density Model. *IUCrJ.* **2020**, 7 (5), 920–933.
- (31) Batke, K.; Eickerling, G. Relativistic Effects on X-Ray Structure Factors. *Phys. Scr.* **2016**, 91 (4), 043010.
- (32) Bučinský, L.; Jayatilaka, D.; Grabowsky, S. Importance of Relativistic Effects and Electron Correlation in Structure Factors and Electron Density of Diphenyl Mercury and Triphenyl Bismuth. *J. Phys. Chem. A* **2016**, 120 (33), 6650–6669.
- (33) Bučinský, L.; Jayatilaka, D.; Grabowsky, S. Relativistic Quantum Crystallography of Diphenyl- and Dicyanomercure. Theoretical Structure Factors and Hirshfeld Atom Refinement. *Acta Cryst. A* **2019**, 75 (5), 705–717.
- (34) Pawłędzio, S.; Malinska, M.; Wońska, M.; Wojciechowski, J.; Malaspina, L. A.; Kleemiss, F.; Grabowsky, S.; Woźniak, K. Relativistic Hirshfeld Atom Refinement of an Organo-Gold(I) Compound. *IUCrJ.* **2021**, 8 (4), 608–620.
- (35) Fang, H.; Zhang, X.-G.; Wang, S.-G. Density Functional Study of Auophilic Interaction in $[X(AuPH_3)_2]^{2+}$ ($X = F, Cl, Br, I$). *Phys. Chem. Chem. Phys.* **2009**, 11 (27), 5796–5804.
- (36) Pyykkö, P.; Xiong, X.-G.; Li, J. Auophilic Attractions between a Closed-Shell Molecule and a Gold Cluster. *Faraday Discuss.* **2011**, 152, 169–178.
- (37) Blake, A. J.; Donamaria, R.; Lippolis, V.; López-de-Luzuriaga, J. M.; Monge, M.; Olmos, M. E.; Seal, A.; Weinstein, J. A. Unequivocal Experimental Evidence of the Relationship between Emission Energies and Auophilic Interactions. *Inorg. Chem.* **2019**, 58 (8), 4954–4961.
- (38) Andrejić, M.; Mata, R. A. Study of Ligand Effects in Auophilic Interactions Using Local Correlation Methods. *Phys. Chem. Chem. Phys.* **2013**, 15 (41), 18115–18122.
- (39) Wang, S.-G.; Schwarz, W. H. E. Quasi-Relativistic Density Functional Study of Auophilic Interactions. *J. Am. Chem. Soc.* **2004**, 126 (4), 1266–1276.
- (40) Pinter, B.; Broeckert, L.; Turek, J.; Růžička, A.; De Proft, F. Dimers of N-Heterocyclic Carbene Copper, Silver, and Gold Halides: Probing Metallophilic Interactions through Electron Density Based Concepts. *Chem. Eur. J.* **2014**, 20 (3), 734–744.
- (41) Kleemiss, F.; Dolomanov, O. V.; Bodensteiner, M.; Peyerimhoff, N.; Midgley, L.; Bourhis, L. J.; Genoni, A.; Malaspina, L. A.; Jayatilaka, D.; Spencer, J. L.; White, F.; Grundkötter-Stock, B.; Steinhauer, S.; Lentz, D.; Puschmann, H.; Grabowsky, S. Accurate Crystal Structures and Chemical Properties from NoSpherA2. *Chem. Sci.* **2021**, 12 (5), 1675–1692.
- (42) Bader, R. F. W. Atoms in Molecules: A Quantum Theory. *International Series of Monographs on Chemistry*; Oxford University Press: Oxford, NY, 1994.
- (43) Jones, P. G.; Lautner, J. Chloro(Dimethyl Sulfide)Gold(I). *Acta Cryst. C* **1988**, 44 (12), 2089–2091.
- (44) Pal, R.; Mebs, S.; Shi, M. W.; Jayatilaka, D.; Krzeszczakowska, J. M.; Malaspina, L. A.; Wiecko, M.; Luger, P.; Hesse, M.; Chen, Y.-S.; Beckmann, J.; Grabowsky, S. Linear $MgCp^*_2$ vs Bent $CaCp^*_2$: London Dispersion, Ligand-Induced Charge Localizations, and Pseudo-Pregostic C–H...Ca Interactions. *Inorg. Chem.* **2018**, 57 (9), 4906–4920.
- (45) O'Connor, A. E.; Mirzadeh, N.; Bhargava, S. K.; Easun, T. L.; Schröder, M.; Blake, A. J. Auophilicity under Pressure: A Combined Crystallographic and in Situ Spectroscopic Study. *Chem. Commun.* **2016**, 52 (41), 6769–6772.
- (46) Hapka, M.; Dranka, M.; Orłowska, K.; Chalaśiński, G.; Szczyński, M. M.; Zachara, J. Noncovalent Interactions Determine the Conformation of Auophilic Complexes with 2-Mercapto-4-Methyl-5-Thiazoleacetic Acid Ligands. *Dalton Trans.* **2015**, 44 (30), 13641–13650.